Adsorption of monovalent and divalent cations on planar water-silica interfaces studied by optical reflectivity and Monte Carlo simulations

Maria Porus, Christophe Labbez, Plinio Maroni, Michal Borkovec

July 8, 2011

Adsorption of Monovalent and Divalent Cations on Planar Water-Silica Interfaces Studied by Optical Reflectivity and Monte Carlo Simulations

Maria Porus[1], Christophe Labbez[2], Plinio Maroni[1], Michal Borkovec[1,*]

[1]Department of Inorganic, Analytical and Applied Chemistry, Geneva University, CH-1205 Geneva, Switzerland.

[2]Laboratoire Interdisciplinaire Carnot de Bourgogne, UNR 5209 CNRS, Université de Bourgogne, F-21078 Dijon, France.

*Corresponding author. Email. michal.borkovec@unige.ch

Abstract

Adsorption on planar silica substrates of various monovalent and divalent cations from aqueous solution is studied by optical reflectivity. The adsorbed amount is extracted by means of a thin slab model. The experimental data are compared with grand canonical Monte Carlo titration simulations at the primitive model level. The surface excess of charge due to adsorbed cations is found to increase with pH and salt concentration as a result of the progressive dissociation of silanol groups as inferred from simulations. The simulations predict, in agreement with experiments, that the surface excess of charge from divalent ions is much larger than from monovalent ions. Ion-ion correlations explain quantitatively the enhancement of surface ionization by multivalent cations. On the other hand, the combination of experimental and simulation results suggests the possibility for the existence of a second ionizable site in the acidic region. Variation of the distance of closest approach between the ions and surface sites captures ion specificity of water-silica interfaces.

Graphical Abstract

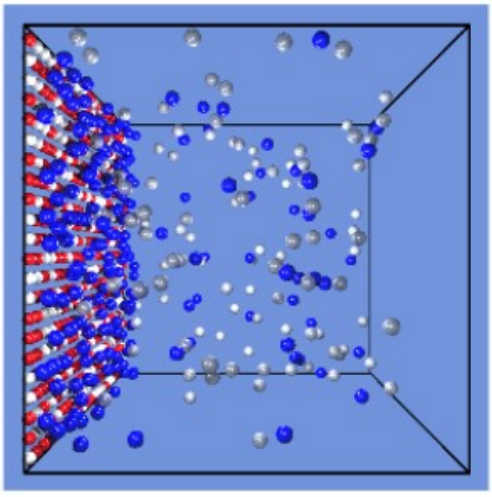

Introduction

Interfaces between water and most other media are charged. Examples include air-water interfaces,[1-4] oil-water interfaces, mercury-water interfaces, or solid-water interfaces involving metals, polymers, clays, or oxides.[15-22] The sign and magnitude of the surface charge density has important consequences in a wide number of applications, including water purification, papermaking, or mineral processing. In water purification[23] or papermaking,[24] multivalent ions or polyelectrolytes are being added to neutralize the particle charge and to induce aggregation. In mineral processing, various minerals can be separated by flotation through differences in their surface charge.[25]

The surface charge accumulates through three main mechanisms, namely ion adsorption, ion substitution, and ionization of surface groups. Apparently neutral surfaces such as air, oil, or metals acquire a charge through preferential adsorption of particular ions from solution.[3] Since anions often adsorb more strongly to neutral surfaces than cations, many surfaces are negatively charged. Clay minerals acquire their charge by isomorphous substitution of silicon and aluminium atoms by metal ions of lower charge, leading to a negative charge of the crystal.[14] Finally, reactive surface moieties, such as hydroxide, carboxylic, or amine groups, may ionize by dissociation or adsorption of protons, leading to the buildup of a surface charge. The archetypal process is the ionization of the silanol group

$$\mathrm{Si-OH} \quad \bar{\tau} \quad \mathrm{Si-O^- + H^+}$$

occurring on surfaces of silica, glass, quartz, or clay minerals. While this reaction is the principal origin of the surface charge, other types of dissociable sites may also contribute (see Figure 1a). This dissociation mechanism on a silica surface will be addressed in this article.

Such dissociation reaction equilibria at water-oxide interfaces were studied in substantial detail in geochemistry, environmental chemistry, and materials processing. These systems are normally investigated as suspensions of colloidal particles with batch depletion experiments and potentiometric titration techniques. The reaction equilibria are typically treated with so-called surface complexation models. Such models are based on mass action laws and capacitive terms accounting for the charging of the electrical double layer. The latter is described within the mean

field approximation of the primitive model (PM) by means of the Poisson-Boltzmann (PB) equation whereby all correlations between the ions are neglected. Monovalent counterions are normally treated as inert, except that their finite distance of approach to the surface is approximated by means of an effective capacitance. Divalent counterions do often interact with the interface more strongly, and they are assumed to form coordination complexes with the reactive surface groups.[26] While such classical surface complexation models have reached substantial maturity, they have retained a certain degree of empiricism. Their origin from a more microscopic picture remains unclear. Some time ago it was shown that surface complexation models can be derived from a mean-field approximation of the underlying dissociation process of the surface sites, in analogy to the lattice approach used to treat gas adsorption equilibria.[31]

More recently, ionization equilibria have been treated within the full PM of electrolyte solutions, where ion-ion correlations are explicitly considered by representing the ions and titratable surface sites as charged hard spheres. Such models can be solved exactly with Monte Carlo (MC) simulations or approximately by integral equations. While the PB equation is known to provide an accurate description of monovalent salt solution even in the close proximity of relatively highly charged surfaces, the PB equation breaks down at comparable conditions for multivalent ions due to the neglect of ion-ion correlations. Given these limitations, any treatment of the adsorption of multivalent ions relying on the PB approximation must be considered as questionable. The commonly introduced coordination complexes of multivalent ions might actually represent an artifact due to the neglect of ion-ion correlation inherent to the PB approximation, or at least partially.

The present study addresses differences in the adsorption between monovalent and divalent cations on water-silica interfaces with the PM and MC simulation techniques. Such systems are normally investigated experimentally in particle slurries, but the interpretation of such experiment is always complicated by the presence of various crystal faces or eventual micro-porosity of the particles. Here we propose an alternative approach freed of such difficulties, where adsorption of cations is studied on a well-defined planar surface with an optical reflectivity technique in situ.[36] In our view, the combination of these two techniques has a substantial potential to study adsorption processes at water-mineral interfaces on a much more microscopic level than it was possible so far.

Monte Carlo Simulations of the Primitive Model

The interface is modeled with a planar surface with discrete titratable sites, which are in equilibrium with a salt solution. The surface consists of an infinite planar wall decorated by titratable sites arranged on a square lattice (see Figure 1b). The surface sites are modeled as hard spheres with diameter d_s. The electrolyte solution is described by the restricted PM, whereby any charged ion i with valence z_i is treated as a hard sphere of diameter d. The solvent is characterized only by a continuum dielectric permittivity ε_s that is also assigned to the interior of ions and sites. The entire system is placed in a cubic box forming a slab. The simulation box, which is overall electroneutral, is then composed of one titrating surface in contact with a salt solution. The concentration of the latter is imposed by the equilibrium with a bulk in a grand canonical procedure. The system is modeled with periodic boundary conditions in the two dimensions parallel to the surface and has a finite size perpendicular to the surface. In that direction, the simulation box is closed by a neutral impenetrable wall. Although the approach is quite general, the model parameters are chosen here to represent silica surfaces.

The interaction between two charged species of valency z_i, z_j located at positions r_i, r_j, is described by an electrostatic potential energy,

$$u^{el}\left(r_{ij}\right) = \frac{z_i z_j e^2}{4\pi\varepsilon_0\varepsilon_s r_{ij}}$$

where e is the elementary charge and ε_0 the permittivity of vacuum, and a short range hard-core repulsion

$$u^{hs}\left(r_{ij}\right) = \begin{cases} \infty & \text{for } r_{ij} < d \\ 0 & \text{for } r_{ij} > d \end{cases}$$

We use the standard Metropolis algorithm.[37] The calculations are performed in the grand canonical ensemble (μVT), whereby the ionic species in the simulation cell are in equilibrium with those in an infinite bulk solution. The chemical potentials of the bulk solution of the desired salt concentration are calculated in a separate simulation with the Widom method. Monovalent

and divalent salt solutions were studied with a concentration range from 1 to 1000 mM. The temperature was set to 298 K and the solvent dielectric constant was taken to be $\varepsilon_s = 78.7$. A common diameter of $d = 4$ Å was assigned to each ion in solution.

In the simulations the surface site density of 4.8 nm^{-2} was used.[33] The dimensions of the simulation box were chosen large enough to ensure that the number of ions was higher than 300 and the properties of the electric double layer at the silica surface were unaffected by the truncation of the system by the neutral wall. A total of 10^5 configurations for each solution ion were sampled in each MC run.

In addition to the classical moves of a grand canonical MC, the surface sites are allowed to dissociate. This reaction can be described with eq. for which the equilibrium constant K is defined as

$$K = \frac{a_{\mathrm{Si-O^-}} a_{\mathrm{H^+}}}{a_{\mathrm{Si-OH}}}$$

where the a_i are the activities of the different species i involved. As commonly used in solution chemistry, we introduce the abbreviations $\mathrm{p}K = -\log_{10} K$ and $\mathrm{pH} = -\log_{10} a_{\mathrm{H^+}}$. In the MC simulations the ionization of the sites corresponds to the change in their charge state, namely 0 when protonated and -1 when deprotonated. The ionization process is modeled in two steps. First, by the release of the proton from the surface site, and then followed by the transfer of the salt pair $\mathrm{H^+}$ and $\mathrm{B^-}$ from the simulation box to the bulk, where $\mathrm{B^-}$ is a salt anion. The corresponding Boltzmann factor for the trial energy is given by

$$\exp(-\beta \Delta U) = \frac{N_{\mathrm{B}}}{V} \exp(-\beta \mu_{\mathrm{B}}) \exp\left(-\beta \Delta U^{el}\right) \exp\left[10(\mathrm{pH} - \mathrm{p}K)\right]$$

where V is the volume of the simulation cell, ΔU^{el} the change in electrostatic energy and μ_{B} and N_B represents the chemical potential and the number of ions $\mathrm{B^-}$, respectively. The protonation is done in the exact reverse order and, thus, the Boltzmann f<actor for the respective trial energy reads

$$\exp(-\beta\Delta U) = \frac{V}{N_B+1}\exp(+\beta\mu_B)\exp\left(-\beta\Delta U^{el}\right)\exp\{\ln 10(\mathrm{pH}-\mathrm{p}K)\}$$

Note that the protons are not explicitly treated but are accounting for through the constant pH. On the other hand, it is easy to demonstrate that the acceptance rules defined from equation (5) and (6) obeyed the detailed balance once one has recognized that they are based on two consecutive grand canonical moves. More details on this simulation methodology are given elsewhere.[32]

The above described method can be extended to surfaces or molecules having different types *i* of site by defining the respective intrinsic dissociation constants $\mathrm{p}K_i$. In the case of silica, experimental studies suggest the existence of two types of silanol groups. This hypothesis will also be tested here. To perform simulations involving different sites, a fraction *f* of the silanols groups were selected randomly and ascribed the intrinsic dissociation constant $\mathrm{p}K_1$. The constant $\mathrm{p}K_2$ was assigned to the remaining silanol sites. To avoid effects of surface specific configurations, various configurations of surface sites were generated during the course of the simulation and the results were averaged. In practice, when the change in the ionization state of an arbitrary site is attempted during the MC move, its ionization constant is randomly assigned to $\mathrm{p}K_1$ with the probability *f* and to $\mathrm{p}K_2$ with the probability 1–*f*.

A distance of closest approach $d_{is} = (d + d_s)/2$ to the surface sites was chosen for each ion *i*.

The distance of closest approach $d_{is} = (d + d_s)/2$ between the surface sites and the ions was used as an adjustable parameter. This quantity was adjusted by choosing the appropriate diameter of the surface site d_s. For Na^+, Ca^{2+} and Mg^{2+}, this distance of closest approach d_{is} was taken from previous work on silica[32] and their respective values are summarized in Table 1. To avoid cumbersome fitting procedures for the other ions, illustrative calculations were performed with d_i = 3Å, 4Å and 5Å. We always use $\mathrm{p}K = 7.7$ for the one-site model. For the two-site model, we use $\mathrm{p}K_1$ = 4.5 and $\mathrm{p}K_2$ = 8.2 with *f* = 0.09. These values were found by comparison with the experimental data and with the restriction that the charge densities at high pH values (pH > 8)

are nearly identical to the 1 pK model. Nevertheless, they are similar to the ones suggested previous studies (please give the references.

Probing Ion Adsorption by Optical Reflectivity

Adsorption of monovalent and divalent cations on a planar water-silica interface was measured with reflectivity. The silica surfaces were obtained by heating silicon wafers (p-type, Silchem, Germany) for 4 min at 1000°C in air. The wafers were treated for 15 min in a mixture of water, concentrated ammonia (27%), and hydrogen peroxide (30%) in the volume ratio 5:1:1 at 80°C. Subsequently, they were extensively rinsed in water and dried. The typical thickness of the silica layer was about 15 nm as measured by null-ellipsometry in air. All solutions were prepared with Milli-Q water, the salts were obtained from Fluka. The solution pH was adjusted with HCl and NaOH.

The reflectivity setup uses a fixed-angle goniometer and a stagnation point flow cell (Figure 2). The reflectometer uses a stabilized He-Ne laser of a wavelength of 632.8 nm with beam intensity fluctuation smaller than 0.5%. The cell consists of a capped equilateral prism made with a borehole perpendicular to its base, which is kept at a given distance parallel to the wafer through a spacer. The reflected beam is split into parallel (p) and perpendicular (s) components by a polarizing beam-splitter and the two respective beam intensities are monitored with two optical diodes with a lock-in detection scheme. The ratio of these two intensities represents the reflectometry signal R. KCl as background electrolyte was not investigated in detail, as it leads to an unstable reflectometry signal. Further details on the reflectometry setup can be found elsewhere.

The time-dependent signal is normalized to its initial value $R(0)$ as

$$S(t) = \frac{R(t) - R(0)}{R(0)}$$

where $t = 0$ corresponds to the beginning of the experiment. The adsorbed mass Γ on the surface is directly proportional to the reflectometry signal

$$\Gamma(t) = \frac{S(t)}{A}$$

The sensitivity factor A is evaluated with Abeles matrix formalism from the homogeneous two-slab model. The refractive index of the layer is calculated from the relation

$$n = n_{\mathrm{W}} + \left(\frac{dn}{dc}\right)_{\mathrm{MCl}_z} c_0 + \left(\frac{dn}{dc}\right)_{\mathrm{M}^{n+}} \frac{\Gamma_{\mathrm{M}^{n+}}}{L}$$

where $(dn/dc)_{\mathrm{MCl}_z}$ and c_0 the refractive index increment and the concentration of the salt solution MCl_z, $(dn/dc)_{\mathrm{M}^{n+}}$ the refractive index increment of the cation M^{n+} and L the thickness of the slab, which was chosen to be two times the Debye length. The results were independent of the slab thickness, provided this parameter was chosen large enough. The contribution of the anions depleted from the surface was found to be negligible. The refractive index increments of the salt in water were measured with a differential refractometer at the same wavelength and are summarized in Table 2. The single refractive index increments were calculated from the mixing relation

$$\left(\frac{dn}{dc}\right)_{\mathrm{MCl}_z} = \left(\frac{dn}{dc}\right)_{\mathrm{M}^{z+}} + z\left(\frac{dn}{dc}\right)_{\mathrm{Cl}^-}$$

with the value of the single refractive index increment $(dn/dc)_{\mathrm{Cl}^-} = 3.1$ mL/mol reported previously.[36] The fact that formation of solution complexes does not interfere with the refractive index and reflectivity measurements was checked with salts involving other anions, in particular nitrates and perchlorates.

Simulation Results

Before comparing simulation and experimental results, general predictions of the PM on the charging process and ion adsorption at titrating surfaces will be presented. Thereby, we focus our attention on the qualitative difference between monovalent and divalent counterions. We first recall briefly results obtained on the surface charge process of silica in salts involving monovalent and divalent cations, and then we present results on the adsorbed excess.

Figure 3a presents the ionization of a water-silica interface as predicted by the PM for the one-site model. The degree of ionization increases with increasing pH due to progressive dissociation of the silanol groups. The dissociation is predicted to be more pronounced for divalent calcium

ions in solution than for monovalent sodium ions. While similar behavior was observed experimentally[20], this behavior was interpreted in terms of specific ion properties. The present simulations predict this behavior purely due to electrostatics, and it can be explained by the so-called charge correlations between the sites and the counterions. These charge correlations were recently shown to explain the increase of the surface charge density of silica particles in presence of divalent ions quantitatively.[32]

Figure 3b shows the same results for the two-site model. In that case, one observes that the surface ionizes already at lower pH. At the same time, divalent cations again promote the ionization of the interface in comparison to monovalent ones. The increase of the charge-correlations and the drop of the entropy of the system (the number of counterions is divided by two) as the counterion valence is raised lead to a larger accumulation of the divalent counterions near the surface. This point is illustrated in the normalized concentration profiles as a function of the distance from the interface for monovalent cations shown in Figure 4 and those of divalent cations shown in Figure 5. The latter figure also illustrates a progressive layering of the multivalent ions near the water-solid interface, which can be evidenced by oscillatory concentration profiles. Charge correlations may further lead to charge reversal as observed on the PM level by MC simulations.[33] The charge reversal was also observed experimentally for silica in the presence of divalent and trivalent cations by streaming potential measurements.[42]

Another way to illustrate the differences between ionization of a water-silica interface in the presence of monovalent and divalent cations is to investigate the adsorbed amount of cations and anions calculated by integration of the concentration profiles. Figure 6 compares the excess surface charge originating from adsorbed cations or anions as a function of the salt concentration at pH 10. One observes that the surface excess of cations increases with increasing salt concentration. The excess charge due to adsorbed divalent counterions is substantially larger than for monovalent ones. For monovalent ions, the coions are always excluded from the interface, and the coion isotherm decreases monotonically with increasing salt concentration. For divalent counterions, however, the coion isotherm is non-monotonic. The isotherm increases at first and decreases only at higher concentrations.

The excess surface charge of the different ions as a function of pH are shown in Figure 7 for the monovalent cation and in Figure 8 for the divalent ones. One observes that the amount of charge

due to divalent cations is much larger than for monovalent ones. However, the concentration dependence is weaker for the divalent ones. Conversely, the amount of coions excluded from the surface is much larger for the monovalent ones. One observes a non-monotonic dependence of the adsorbed coions in the presence of divalent cations (Figure 8b).

Before to start with the comparison between experiments and simulations results, let us give some insight into the non-monotonic dependence of the coions isotherms when counterions are divalent. Upon increasing the 2-1 salt concentration and at high enough pH, Figure 6b, divalent counterions accumulate, just next to the surface (see Figure 5a) faster than the surface charges are formed and, as a response of this increased screening, the coion depletion drops. Upon a threshold value, the accumulation of counterions is strong enough to overcharge the surface which, in turn, results in the accumulation of coions next to the calcium layer, best seen in Figure 5b. Upon further addition of salt, counterion adsorption starts to saturate, see the slop inflection in Figure 5b, which finally leads to the drop of coion adsorption. When the pH is varied, Figure 8b, the scenario is about the same, expect that this time, the coion isotherm starts with a drop before to rise. In this case, the system is initially driven by the entropy (weakely coupled) due to the low pH values (# weak surface charges) and behaves similarly to systems with a 1-1 salt, until the ion-ion correlations takes over, at high enough pH values, where the system then follows the same trend as previously described.

Comparison with Experiment

The adsorbed amount of cations obtained experimentally from reflectivity data will now be compared with the corresponding results from simulations. The experiments have been carried out for a series of monovalent and divalent cations at different pH and salt concentrations. Initially, we will discuss the behavior of sodium and magnesium, as two examples of a monovalent and divalent cation. Subsequently, various types of cations will be compared. The adsorbed amount will be always reported as the surface excess of cation charge expressed as elementary charges per unit area. The simulations have been carried out for the two-site model. Consideration of this model was found to give a satisfactorily description, although no perfect,

for the substantial ion adsorption in the intermediate pH range. The justifications and limitations of the model will be discussed.

Figure 9 shows the adsorbed amount of the monovalent sodium ions from NaCl solution. The pH dependence is shown in Figure 9a, while the salt concentration dependence in Figure 9b. These adsorption isotherms closely resemble the classical charging curves of silica as measured by potentiometric titrations. One observes that the adsorbed amount increases with increasing pH in agreement with simulations. This effect is due to the progressive dissociation of the silanol groups at the interface, which requires an increasing amount of cations to neutralize this charge. One further observes that the adsorbed amount weakly increases with increasing salt concentration at fixed pH. Again, these trends are in line with simulation results. This effect can be explained by the fact that silanol groups dissociate with increasing salt level, which induces a larger screening of the repulsion between the ionized groups.

A qualitatively similar behavior is observed to the divalent cation magnesium as shown in Figure 10. Note that the data were only measured up to pH 8.5 since precipitation occurs at higher pH. Again the adsorbed amount increases with increasing pH and increasing salt concentration. For the divalent cations, however, the adsorbed charge is greatly enhanced with respect to the monovalent cations. This trend is well captured by the MC simulations invoking purely electrostatic interactions. Moreover, these findings support previous results based on a comparison between MC simulations of surface charge and surface potentials with potentiometric titrations of silica slurries and streaming current measurements of silica surfaces.[33] That study reported that divalent cations promote ionization of surface groups and that they strongly accumulate at the interface to the point that the charge can even be reversed. This charge reversal can be explained with ion-ion correlations quantitatively.

A remarkable aspect of the measured adsorption isotherms is the intermediate plateau in the neutral pH region. This plateau is much more pronounced for divalent cations than for the monovalent ones and is also shifted to higher pH for the monovalent ones. This plateau is found to be satisfactorily reproduced by simulations when a second type of silanol site of lower pK is introduced. The classical one-site model predicts the surface charge to be unrealistically low. At higher pH, the calculated surface charge is very similar whether one or two sites are being used. The existence of two types of ionizable sites was also suggested on the basis of studies on planar

silica substrates with reflectivity[36], second harmonic generation, or other spectroscopic techniques.[43-45] Potentiometric titration data of colloidal silica suspensions mostly do not reveal such an intermediate plateau. However, some authors did report comparable deviations with this technique, which could also suggest the existence of a more acidic ionizable site (are you sure references?). This disparate behavior of various silica surfaces suggests that the surface reactivity of these interfaces is different. On precipitated silica the acidic site seems to be absent, while it seems to appear on fused silica. Since it was shown that various silica samples may show different stability behavior,[18] a different adsorption on different silica surface may no longer come as a surprise. The existence of various types of silanol groups was also suggested from ab-initio simulations. In particular, the site of lower acidity was recently suggested to be found in locally strained or defected regions of the silica surface.[28]

Let us now discuss the ion-specificity effects on the adsorbed cation charge. To model the ion-specificity effects within the PM, the minimum approach distance between the cations and the surface sites d_i is being varied. Figure 11 compares various monovalent and divalent cations at pH 7.0, 8.5, and 10.0. At pH 10.0 only data for monovalent cations are presented in Figure 11c, since some of the divalent salt precipitate at this pH. Higher amount of divalent ions adsorbs at pH 7.0. The values are well predicted by simulations, even though the predicted salt dependence is somewhat weaker than experimentally observed. The characteristic difference between monovalent and divalent cations persists at pH 8.5. However, one can see that the actual amount adsorbed now strongly depends on the type of divalent cation. For the monovalent cations, on the other hand, the ion specificity remains weak in agreement with previous experimental studies based on potentiometic titration[20] and second harmonic generation.[49] Furthermore, these ion specific effects at the water-silica interface are well described, at least semi-quantitatively, by the MC simulations through a simple variation of the distance of closest approach d_i. Indeed, the same variation of d_i from 3 to 5 Å allows us to capture the much larger changes in the adsorbed charge observed for the divalent cations than for the monovalent ones. Ion specific effects are magnified for the monovalent cations at pH 10.0, in full agreement with the simulations.

Before to conclude let us discuss the limitations on the model used. Indeed, as can be seen from the comparison between simulations and experimental results, the two sites model presents some

weaknesses in the low salt regime for pH < 8.5 although it satisfactorily captures the observed dependence on pH, in particular the shoulder. The simple parameters used that is the second pK value as well as the variation of d_{is} may, indeed, mask other mechanisms, e.g. surface relaxations, surface polarization, water structuring effects, that could, if correctly treated, better describe the observables. All that to say, that more experimental and theoretical studies would be required to solve the apparent paradox between one silanol type on colloidal silica and two silanol types on large silica surfaces, and, more generally, to give a more detailed understanding on ion adsorption at solid/liquid interfaces. Nevertheless, lacking such molecular details, this simple treatment, through the use of the PM, presents the great advantage to provide the main physics and thus to capture, in a semi-quantitative manner, the main evolutions of the system.

Conclusions

This study demonstrates the feasibility of a novel approach to study adsorption of ions to water-oxide interfaces. The ion adsorption is measured on a planar substrate with a highly-sensitive optical reflectivity technique. The experimental data are then directly compared with MC simulations on the PM level.

Similar information is frequently obtained from studies on colloidal particle slurries and the data are interpreted in terms of surface-complexation models. The advantage of the present approach is twofold. First, the adsorption isotherms are measured on a well-defined substrate, while experimental results obtained in slurries are blurred by the presence of various crystal faces or particle micro-porosity. Second, the PM treats the ion-ion correlations exactly, while surface complexation models invoke a mean-field approximation to treat the electrical double layer. By now it is well established that this approximation breaks down for divalent or multivalent ions.

The present study addresses the adsorption of monovalent alkali and divalent earth-alkali metal cations to the water-silica interface, whereby the surface is obtained by heating a silicon wafer. This interface shows similar adsorption behavior as known from classical potentiometric titration studies, but seems to indicate the existence of two types of silanol sites. Although more theoretical and experimental studies would be require to validate this hypothesis, the existence of

various types of sites on a water-silica interface was inferred on the basis of spectroscopic and computer simulation studies.

The present approach can be extended in various ways. Wide range of well-defined oxide surfaces can be prepared by vapor deposition or epitaxial growth, and such surfaces could be investigated similarly. Since reflectivity is an unspecific technique, other types of ions can be investigated as well. Finally, the simulation technique is perfectly general, and allows the introduction of an atomistic representation of the interface, and more detailed models of the ions. We suspect that the present framework will evolve into a powerful approach on investigate adsorption phenomena at water-oxide interfaces from a much more molecular point of view than currently done.

Acknowledgements

This research was supported by the Swiss National Science Foundation and University for Geneva. CL acknowledges the support of the CRI (Bourgogne University) for access to its computer facility.

References

1. L. Parkinson and J. Ralston, J. Phys. Chem. C **114,** 2273 (2010).
2. K. Hanni-Ciunel, N. Schelero, and R. von Klitzing, Faraday Discuss. **141,** 41 (2009).
3. J. K. Beattie, A. N. Djerdjev, and G. G. Warr, Faraday Discuss. **141,** 31 (2009).
4. A. Graciaa, G. Morel, P. Saulner, J. Lachaise, and R. S. Schechter, J. Colloid Interface Sci. **172,** 131 (1995).
5. K. G. Marinova, R. G. Alargova, N. D. Denkov, O. D. Velev, D. N. Petsev, I. B. Ivanov, and R. P. Borwankar, Langmuir **12,** 2045 (1996).
6. J. Zheng, S. H. Behrens, M. Borkovec, and S. E. Powers, Environ. Sci. Technol. **35,** 2207 (2001).
7. D. C. Grahame and R. Parsons, J. Am. Chem. Soc. **83,** 1291 (1961).
8. A. J. Bard and L. R. Faulkner, *Electrochemical Methods: Fundamentals and Applications* (John Wiley, New York, 2001).
9. D. Barten, J. M. Kleijn, J. Duval, H. P. van Leeuwen, J. Lyklema, and M. A. Cohen Stuart, Langmuir **19,** 1133 (2003).
10. N. Kallay, Z. Torbic, M. Golic, and E. Matijevic, J. Phys. Chem. **95,** 7028 (1991).
11. B. Lovelock, F. Grieser, and T. W. Healy, Langmuir **2,** 443 (1986).
12. S. H. Behrens, D. I. Christl, R. Emmerzael, P. Schurtenberger, and M. Borkovec, Langmuir **16,** 2566 (2000).
13. P. V. Brady, R. T. Cygan, and K. L. Nagy, J. Colloid Interface Sci. **183,** 356 (1996).
14. M. Delhorme, C. Labbez, C. Caillet, and F. Thomas, Langmuir **26,** 9240 (2010).
15. D. F. Evans and H. Wennerstrom, *The Colloidal Domain* (John Wiley, New York, 1999).
16. T. Hiemstra, J. C. M. de Wit, and W. H. van Riemsdijk, J. Colloid Interface Sci. **133,** 105 (1989).
17. C. Labbez, B. Jonsson, I. Pochard, A. Nonat, and B. Cabane, J. Phys. Chem. B **110,** 9219 (2006).
18. M. Kobayashi, M. Skarba, P. Galletto, D. Cakara, and M. Borkovec, J. Colloid Interface Sci. **292,** 139 (2005).
19. M. Schudel, S. H. Behrens, H. Holthoff, R. Kretzschmar, and M. Borkovec, J. Colloid Interface Sci. **196,** 241 (1997).
20. P. M. Dove and C. M. Craven, Geochim. Cosmochim. Acta **69,** 4963 (2005).

21. S. H. Behrens and D. G. Grier, J. Chem. Phys. **115,** 6716 (2001).
22. T. F. Tadros and J. Lyklema, J. Electroanal. Chem. **17,** 267 (1968).
23. B. Bolto and J. Gregory, Water Res. **41,** 2301 (2007).
24. D. Horn and F. Linhart, *Retention aids*. 2nd ed.; Blackie Academic and Professional: London, 1996.
25. J. Ralston, D. Fornasiero, and S. Grano, Pulp and solution chemistry. In *Froth Flotation: A Century of Innovation*, Fuerstenau, M. C.; Jameson, G.; Yoon, R. H., Eds. Society for Mining, Metallurgy, and Exploration, Inc.: Littleton, 2007; pp 227.
26. T. Hiemstra and W. H. Van Riemsdijk, J. Colloid Interface Sci. **301,** 1 (2006).
27. S. W. Ong, X. L. Zhao, and K. B. Eisenthal, Chem. Phys. Lett. **191,** 327 (1992).
28. K. Leung, I. M. B. Nielsen, and L. J. Criscenti, J. Am. Chem. Soc. **131,** 18358 (2009).
29. V. Ostroverkhov, G. A. Waychunas, and Y. R. Shen, Phys. Rev. Lett. **94,** (2005).
30. T. W. Healy and L. R. White, Adv. Colloid Interface Sci. **9,** 303 (1978).
31. M. Borkovec, Langmuir **13,** 2608 (1997).
32. C. Labbez and B. Jonsson, Lect. Notes Comp. Sci. **4699,** 66 (2007).
33. C. Labbez, B. Jonsson, M. Skarba, and M. Borkovec, Langmuir **25,** 7209 (2009).
34. L. Guldbrand, B. Jonsson, H. Wennerstrom, and P. Linse, J. Chem. Phys. **80,** 2221 (1984).
35. B. Svensson, B. Jonsson, and C. E. Woodward, J. Phys. Chem. **94,** 2105 (1990).
36. M. Porus, P. Maroni, and M. Borkovec, Sens. Actuators B **151,** 250 (2010).
37. N. Metropolis, A. W. Rosenbluth, M. N. Rosenbluth, A. H. Teller, and E. Teller, J. Chem. Phys. **21,** 1087 (1953).
38. B. Widom, J. Chem. Phys. **39,** 2808 (1963).
39. J. P. Valleau and L. K. Cohen, J. Chem. Phys. **72,** 5935 (1980).
40. L. H. Allen, Matijevi.E, and L. Meties, J. Inorg. Nucl. Chem. **33,** 1293 (1971).
41. J. Kleimann, G. Lecoultre, G. Papastavrou, S. Jeanneret, P. Galletto, G. J. M. Koper, and M. Borkovec, J. Colloid Interface Sci. **303** 460 (2006).
42. F. H. J. van der Heyden, D. Stein, K. Besteman, S. G. Lemay, and C. Dekker, Phys. Rev. Lett. **96,** 224502 (2006).
43. J. D. Fisk, R. Batten, G. Jones, J. P. O'Reilly, and A. M. Shaw, J. Phys. Chem. B **109,** 14475 (2005).

44. J. P. O'Reilly, C. P. Butts, I. A. I'Anson, and A. M. Shaw, J. Am. Chem. Soc. **127,** 1632 (2005).
45. H. F. Fan, F. P. Li, R. N. Zare, and K. C. Lin, Anal. Chem. **79,** 3654 (2007).
46. J. Sonnefeld, A. Gobel, and W. Vogelsberger, Colloid Polym. Sci. **273,** 926 (1995).
47. A. A. Hassanali and S. J. Singer, J. Phys. Chem. B **111,** 11181 (2007).
48. A. A. Skelton, P. Fenter, J. D. Kubicki, D. J. Wesolowski, and P. T. Cummings, J. Phys. Chem. C **115,** 2076 (2011).
49. Z. Yang, Q. F. Li, and K. C. Chou, J. Phys. Chem. C **113,** 8201 (2009).

Table 1. Minimum separation between sites and ions as used in MC simulations.[32]

Distance of closest approach (Å)	Na^+	Ca^{2+}	Mg^{2+}
d_i	3.5	3.5	3.1

Table 2. Refractive index increments of various salt solutions at 633 nm.

Salt	mL/mol	Salt	mL/mol
LiCl	8.91	$MgCl_2$	20.82
NaCl	10.17	$CaCl_2$	23.59
RbCl	11.49	$SrCl_2$	27.09
CsCl	12.96	$BaCl_2$	28.35

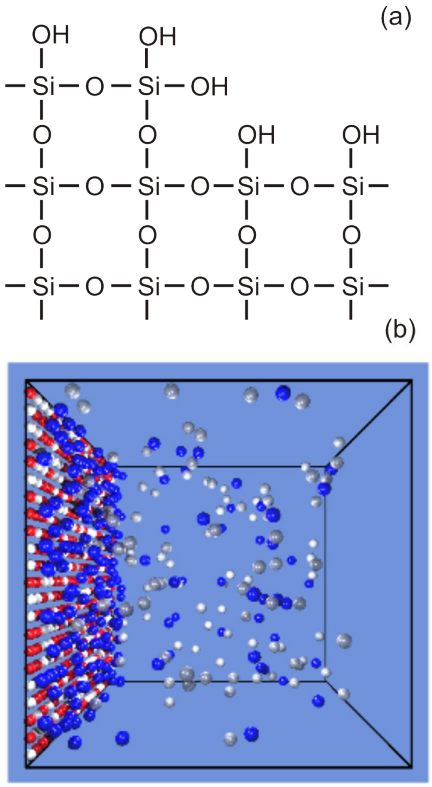

Figure 1. (a) Scheme of the surface termination of a water-silica interface. Note the potential presence of different surface groups. (b) Snapshot of a MC simulation box used to model a water-silica interface in a salt solution. The titrating sites are arranged on a square lattice and may dissociate according to the solution pH and composition.

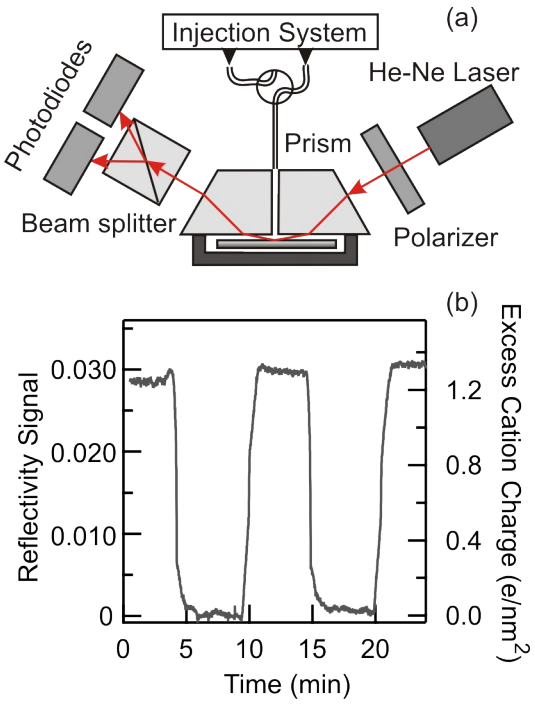

Figure 2. Probing ion adsorption by optical reflectivity. (a) Scheme of the experiment setup. (b) Typical experimental trace of a change between pH 10.2 and 3.0 in 200 mM NaCl solution.

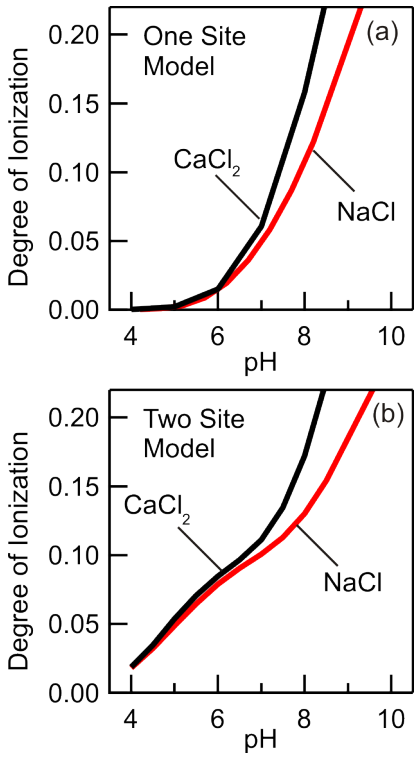

Figure 3. Calculated degree of ionization for water-silica interface in contact with a sodium and calcium salt solution at a constant ionic strength of 200 mM. The MC simulations use a distance of closes approach of $d_i = 3.5$ Å and a site density of 4.8 nm^{-2}. (a) One-site model with $pK = 7.7$, and (b) a two-site model with 9% of sites with $pK_1 = 4.5$ and 91% with $pK_2 = 8.2$.

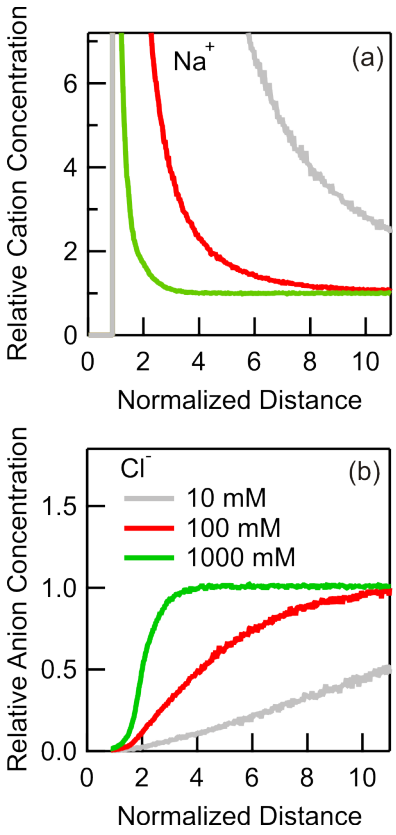

Figure 4. Calculated concentration profiles of ions near a water-silica interface at different concentrations in the presence of a salt with monovalent cations and pH 10. The concentrations are normalized with respect to the respective bulk concentrations and the distances from the surface with respect to the ion diameter $d = 4$ Å. The MC simulations are carried out for the one-site model and they use the same parameters as in Figure 3a. Profiles for (a) cations and (b) anions.

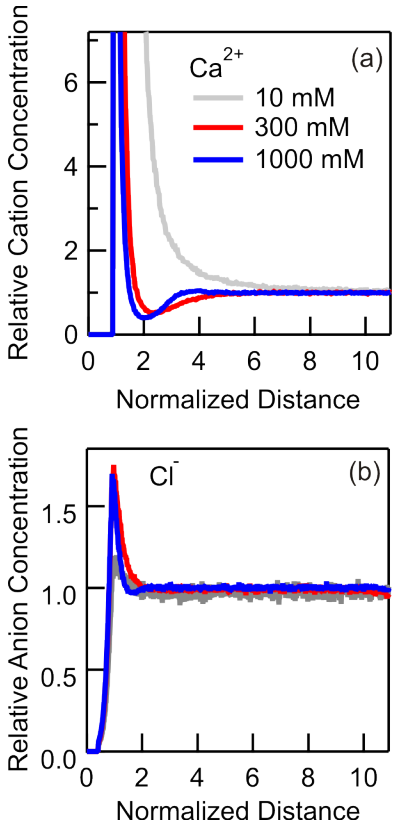

Figure 5. Calculated concentration profiles of ions near a water-silica interface at different concentrations in the presence of a salt with divalent cations and pH 10. The concentrations are normalized with respect to the respective bulk concentrations and the distances with respect to the ion diameter d = 4 Å. The MC simulations are carried out for the one-site model and they use same parameters as in Figure 3a. Profiles for (a) cations and (b) anions.

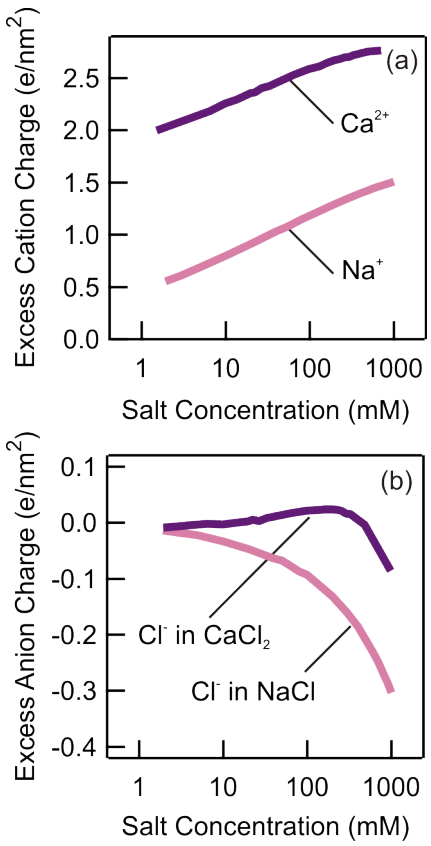

Figure 6. Calculated adsorbed excess ionic charge at a water-silica interface in the presence of a salt with divalent cations and pH 10. The adsorbed amount is expressed as charge due to the adsorbed ions per unit area. The MC simulations are carried out for the one-site model and they use the same parameters as in Figure 3a. Profiles for (a) cations and (b) anions.

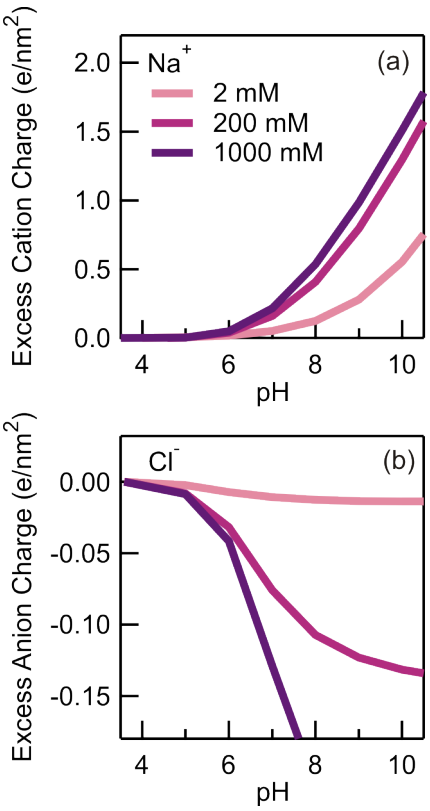

Figure 7. Calculated adsorbed excess ionic charge at a water-silica interface as a function of pH in the presence of a salt with monovalent cations. The adsorbed amount is expressed as charge due to the adsorbed ions per unit area. The MC simulations are carried out for the one-site model and they use the same parameters as in Figure 3a. Profiles for (a) cations and (b) anions.

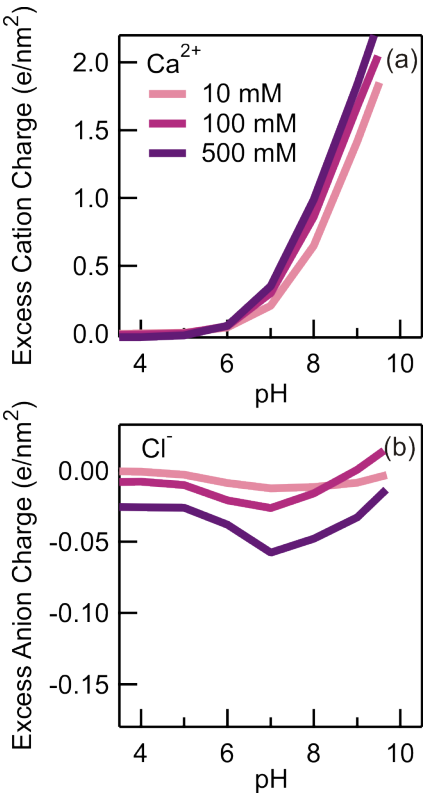

Figure 8. Calculated adsorbed excess ionic charge at a water-silica interface as a function of pH in the presence of a salt with divalent cations. The adsorbed amount is expressed as charge due to the adsorbed ions per unit area. The MC simulations are carried out for the one-site model and they use same parameters as in Figure 3a. Profiles for (a) cations and (b) anions.

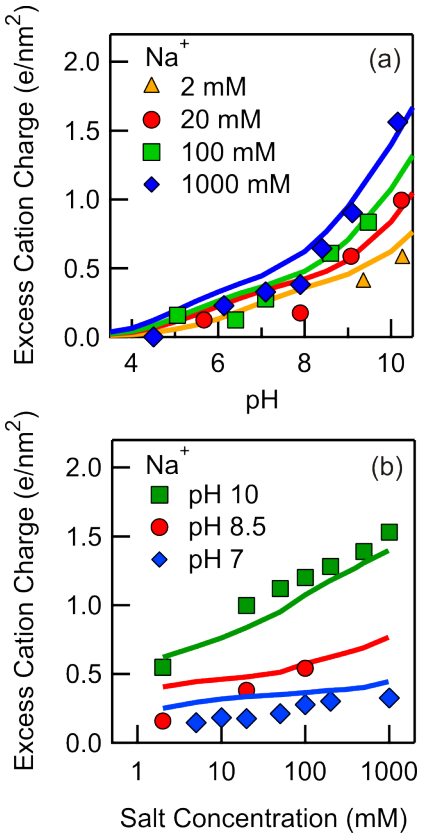

Figure 9. Comparison of experimental (points) and simulations (lines) of the adsorbed excess sodium ion charge at water-silica interface from NaCl solutions. (a) Dependence on pH for different salt concentrations, and (b) dependence on the salt concentration for different pH values.

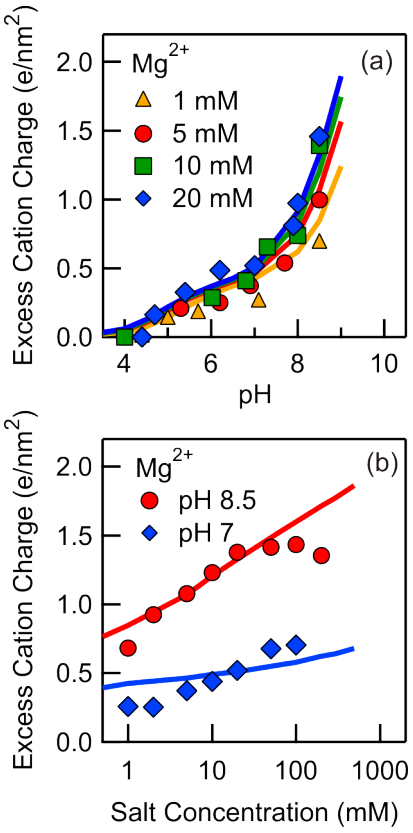

Figure 10. Comparison of experimental (points) and simulations (lines) of adsorbed excess magnesium ion charge at water-silica interface from $MgCl_2$ solutions. (a) Dependence on pH for different salt concentrations, and (b) dependence on the salt concentration for different pH values.

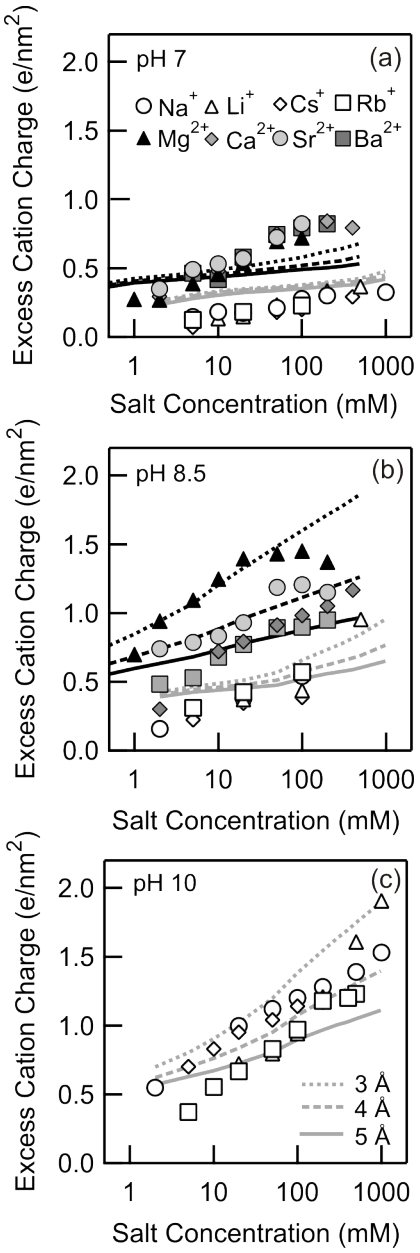

Figure 11. Comparison of experimental (points) and simulations (lines) of the adsorbed excess cation charge at water-silica interface as a function of the salt concentration. The dotted lines indicate results with different distance of closest approach d_i as indicated. (a) pH 7, (b) pH 8.5 and (c) pH 10.0.